Biochimica et Biophysica Acta, 514 (1978) 239—254

BBA 78211

THE STRUCTURE OF ORIENTED SPHINGOMYELIN BILAYERS

R.S. KHARE * and C.R. WORTHINGTON

Departments of Biological Sciences and Physics, Carnegie-Mellon University, Pittsburgh, Pa. 15213 (U.S.A.)

(Received April 12th, 1978)

Summary

X-ray diffraction from oriented bilayers of sphingomyelin gave up to 14 orders of diffraction of a lamellar repeat of 68.5 Å on the meridian and up to eight reflections, including a strong reflection at 4.2 Å, on the equator. The diffraction spacings did not change when the sphingomyelin bilayers were exposed to different humidities. A direct analysis of the low resolution X-ray data, using deconvolution is presented. A comparison of the Patterson functions of sphingomyelin with those of phosphatidylcholine and phosphatidylethanolamine suggests that the molecular structure of sphingomyelin in oriented bilayers resembles the structure of both phosphatidylcholine and phosphatidylethanolamine. Molecular model calculations for sphingomyelin bilayers have also been performed. Electron density profiles of sphingomyelin bilayers at resolution of about 6 Å and about 2.5 Å are presented. Our results indicate that the phosphorylcholine head group of sphingomyelin is in the plane of the membrane and at right angles to the hydrocarbon chains, the hydrocarbon chains are nearly parallel to each other, and there is only a limited, if any, interdigitation of the hydrocarbon chains of the adjacent sphingomyelin molecules in the bilayer.

Introduction

Sphingomyelin is an important constituent of many biological membranes and in particular nerve myelin [1] and is considered to be a structural lipid in membrane [2]. Sphingomyelin has the same phosphorylcholine polar group as phosphatidylcholine and can replace phosphatidylcholine in some membranes such as erythrocyte membranes [3]. Thus the association of sphingomyelin

* Present address: Johnson Space Center, Houston, Texas 77058, U.S.A.
Abbreviation: DMOAP, *N,N*-dimethyl-*N*-octadecyl-1,3-amino-propyl-trismethoxysilyl chloride.

and its interaction with other biological molecules, for instance cholesterol, may be similar to that of phosphatidylcholine. However, the molecular structure of sphingomyelin and phosphatidylcholine are different, for the polar region of phosphatidylcholine contains two ester bonds whereas that of sphingomyelin contains an amide bond, a hydroxyl group and a trans double bond [1]. In the hydrophobic region the average number of CH_2 units in phosphatidylcholine is less that in sphingomyelin, and the difference in the lengths of the two hydrocarbon chains is more pronounced in sphingomyelin than in phosphatidylcholine. There are differences in the net dipole moments of phosphatidylcholine and sphingomyelin and in their ability to form hydrogen bonds [4,5]. These differences between sphingomyelin and phosphatidylcholine are expected to exert specific effects on the structure and association of their bilayers and their interactions with other biolobical molecules. In fact, the phase behaviour [6,7] and the dynamical properties [8] of sphingomyelin are different from those of phosphatidylcholine [8,9]. Recently we have reported differences in the interaction of cholesterol with sphingomyelin and phosphatidylcholine [10].

A number of X-ray diffraction studies have been made on oriented phosphatidylcholine [11—16], and phosphatidylethanolamine [17—19] bilayers but only a few studies on unoriented sphingomyelin bilayers have been reported [20—23]. In this paper a study of the molecular structure of oriented sphingomyelin bilayers using X-ray diffraction is described. A brief account of this work has been previously reported [24].

Materials and Methods

Bovine brain sphingomyelin was obtained from Sigma Chemical Co. and was used without further purification. Oriented samples of sphingomyelin were obtained by slow evaporation of a solution of sphingomyelin in chloroform in glass capillaries (1.0 mm diameter). The inner surfaces of the glass capillaries were coated with a monolayer of the silane surface coupling agent *N,N*-dimethyl-*N*-actadecyl-1,3-amino-propyltrismethoxysilyl chloride (DMOAP) (Dow Corning No. XZ-2-2300). The use of silane coupling agents for orienting lecithin bilayers has been previously described [10]. The silane coupling agent constrains the sphingomyelin molecules to align fairly uniformly normal to the surface of the capillary as shown by their X-ray diffraction patterns.

The X-ray source was a Jarrell-Ash microfocus tube. Some of the patterns were also recorded using Philips microfocus X-ray tube. X-ray diffraction patterns were recorded using an optically focusing X-ray camera [25]. Most patterns were recorded using a point focus collimation, which was obtained by using only one mirror and a guard slit collimation. A specimen-to-film distance of about 7.5 cm or 10 cm was generally used. The X-ray patterns were taken with Ni-filtered CuKα radiation ($\lambda = 1.54$ Å) and were recorded on Ilford industrial G X-ray films. The exposure times varied from 0.5 h for the first few orders to 30 h for the higher orders. The spacings (d) were calculated from the Bragg's equation $2d \sin \theta = h\lambda$, where h is the diffraction order.

Densitometer traces of the patterns were obtained using a microdensitometer (Joyce-Loebl MK-IIIC). The background curve was subtracted from the tracing

in the usual way. The integrated intensities $I(h)$ of the lamellar reflections on the meridian were obtained by measuring the area under the diffraction peaks.

In an attempt to swell sphingomyelin bilayers, oriented samples of sphingomyelin inside the capillary were exposed to various humidities for extended periods of up to 10 days. Different humidities were obtained by using saturated salt solutions. All experiments were carried out at room temperature (20 ± 2°C).

In the analysis of the lamellar reflections that follows, $t(x)$ is the electron density of the unit cell of width d, and $T(X)$ is the Fourier transform of $t(x)$, where x and X are distances in real and reciprocal space, respectively. When the oriented sphingomyelin bilayers have a regular lamellar repeating unit, discrete reflections at $X = h/d$, h is an integer, are recorded. The observed Fourier transform $T_{obs}(h)$, of the bilayers is related to the integrated intensity by the relation [26]:

$$|T_{obs}(h)|^2 = h^2 I(h)$$

Different sets of X-ray diffraction data from sphingomyelin and other lipid bilayers were normalized by using the relation [28]:

$$(2/d) \sum_{h=1}^{h=h_{max}} |T_{obs}(h)|^2 = \text{a constant}$$

The low-angle X-ray data have a minimum spacing of $d(h_{max})^{-1}$ and the X-ray data have a resolution of $d(2h_{max})^{-1}$.

Results

X-ray diffraction patterns obtained from sphingomyelin bilayers are shown in Figs. 1A and 1B. The patterns showed both meridional and equatorial reflections. 14 orders of lamellar reflections of d = 68.5 Å were visible in the original negative. A strong 4.2 Å equatorial reflection is visible in Fig. 1B and other equatorial reflections are also visible in this reproduction. These patterns clearly indicate that our specimens had an oriented lamellar structure. The meridional reflections arise from the regular electron density distribution $t(x)$ along the lamellar repeat. The first six reflections, h = 1—6, have strong intensity while the h = 11—14 reflections have relatively weak intensity. The diffraction data d = 68.5 Å, h = 14, have a resolution of 2.5 Å. The lamellar repeat distance d = 68.5 ± 0.5 Å did not vary when the specimens were placed in high or low relative humidities.

The equatorial reflections derive from the molecular organization in the plane of the bilayers. Eight equatorial reflections at spacings of 12.9, 10.3, 8.9, 8.6, 4.9, 4.2, 3.5 and 3.1 Å were visible on the original negative. The strong wide-angle reflection of 4.2 Å is the usually observed reflection in crystalline-type hydrocarbons and arises from the regular packing of the hydrocarbon chains. A weak and broad diffraction maximum at a Bragg spacing of about 8 Å was also present.

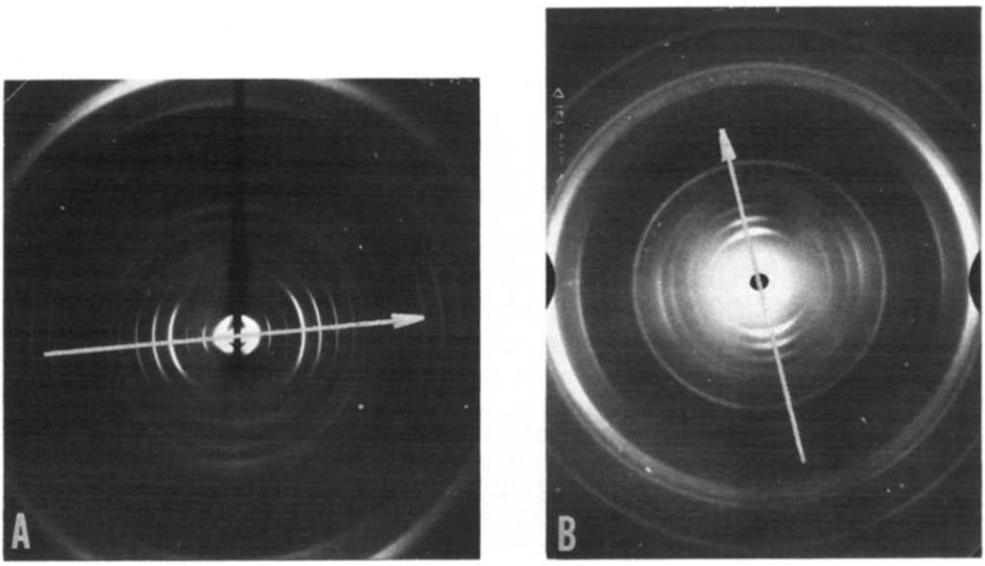

Fig. 1 (A) Low-angle X-ray diffraction pattern of oriented sphingomyelin bilayers. 14 orders of d = 68.5 Å along the meridian, which is indicated by a white arrow, can be seen in the original negative and many of these can be seen in the reproduction. (B) Wide-angle X-ray diffraction pattern of oriented sphingomyelin bilayers. The meridional direction is indicated by a white arrow. The reproduction shows the presence of many non-lamellar reflections and a strong 4.2 Å reflection which is arced on the equator.

Analysis

Oriented specimens of sphingomyelin can be considered to be one-dimensional structures with a center of symmetry. The structure analysis of lamellar diffraction from such bilayers essentially means determination of the phases of the diffraction orders. The one-dimensional electron density profile of the sphingomyelin bilayer as a function of depth along the length of bilayer can be computed once the phases are assigned to the diffraction orders. In the centrosymmetric case, where the phases can only be + or —, one has to select the correct set of phases from the 2^h possible sets, where h is the number of reflections. Sphingomyelin-oriented bilayers showed no swelling in an environment of high relative humidity and therefore we do not have a continuous intensity transform for analysis.

The present analysis is limited to the lamellar diffraction data and was carried out in two stages, the low resolution analysis and the high resolution analysis. The low resolution data, h = 1—6, were analyzed using electron density strip models which were based on the chemical knowledge of sphingomyelin and by a direct deconvolution analysis of the Patterson function. A comparison of Patterson function of sphingomyelin with the Patterson functions of phosphatidylcholine and phosphatidylethanolamine indicated that the polar group of sphingomyelin is in a folded conformation. The high resolution data, h = 1—14, were analyzed using molecular model building.

(A) Low resolution analysis

(1) Electron density strip models. The structural formula for sphingomyelin

Scheme I.

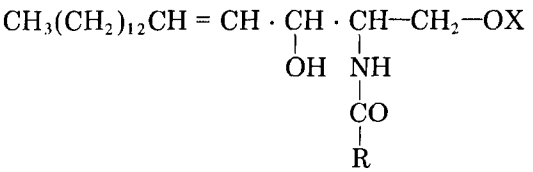

where X is

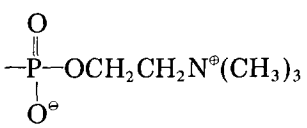

is given in Scheme I. Sphingomyelin has an 18-carbon sphingosine chain and an amide-linked fatty acid (R). Natural sphingomyelin contains a range of fatty acid chains from C_{16} to C_{25} but the composition is dominated by two fatty acid species C_{18} and C_{24} [6,27]. The phosphorylcholine group in fully extended conformation will be about 12 Å and in its folded configuration about 6 Å long. The amide-linked fatty acid chain in fully extended conformation will be about 22—30 Å long. Thus, it appears that the observed spacing of 68.5 Å is the correct order of magnitude to represent twice the molecular length of the sphingomyelin molecule. This chemical information was used to postulate the electron density strip models for the sphingomyelin bilayers.

The use of uniform electron density strip models [28] has proved useful in treating the phase problem in the studies of nerve myelin and photoreceptor membranes [29] and as a first step, this approach was used with lamellar X-ray diffraction data of sphingomyelin bilayers. Using low resolution data, $h_{max} = 6$, uniform electron density strip models [28] were postulated and the calculated Fourier transform values, $T_c(h)$, were compared with the experimental values $T_{obs}(h)$, and a R value defined as

$$R = \frac{\sum_{h=1}^{h=h_{max}} ||T_{obs}(h)| - |T_c(h)||}{\sum_{h=1}^{h=h_{max}} |T_{obs}(h)|}$$

was computed. Electron density strip models with interlocking (model A) and open (model B) packing of hydrocarbon chains were considered. The model parameters which gave minimum R values are shown in Fig. 2. The Fourier transform values derived from the strip models are compared with the observed amplitudes and are listed in Table I. Model A which has interdigitated chains gave a minimum R value of 29%. Model B which has no interdigitation gave a minimum R value of 3%. This comparison leads to the conclusion that the hydrocarbon chains in sphingomyelin bilayers have at most only a limited inter-

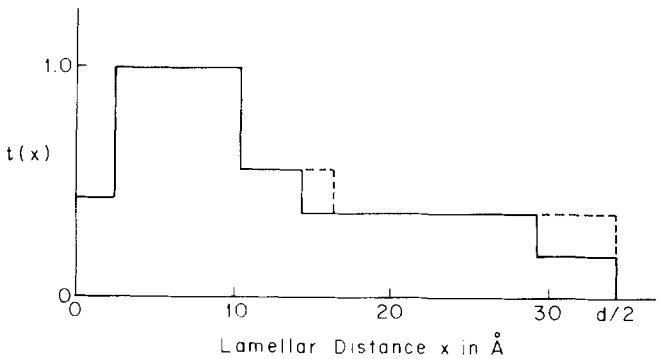

Fig. 2. Electron density strip models of sphingomyelin bilayers. Model B is shown as a solid line and model A when different from model B is shown as a dotted line. Model A has interdigitated hydrocarbon chains whereas model B has only limited interdigitation of hydrocarbon chains.

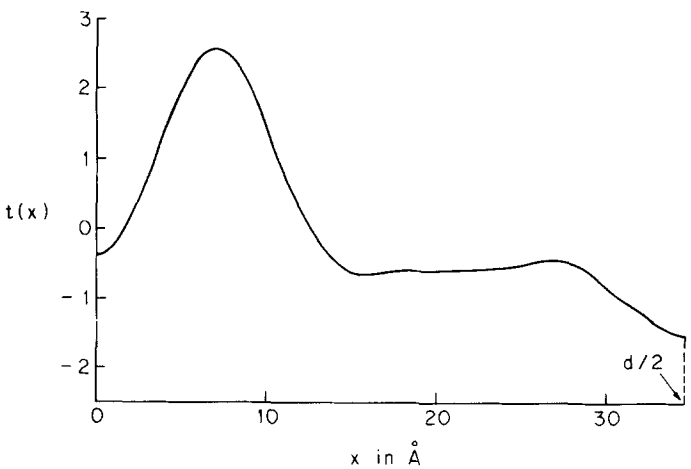

Fig. 3. Electron density profile of sphingomyelin bilayers computed using the first six orders of diffraction and (+, +, —, —, —, —) phases. The Fourier synthesis has a resolution of about 6 Å and the electron density is on a relative scale.

TABLE I

THE OBSERVED AND CALCULATED FOURIER TRANSFORM VALUES FOR SPHINGOMYELIN BILAYERS

The calculated values were derived from the strip models in Fig. 2.

	h					
	1	2	3	4	5	6
$\|T_{obs}(h)\|$	4.12	0.74	0.55	2.74	1.56	1.36
$T_c^*(h)$	+3.87	+1.22	—1.82	—2.05	—1.87	—1.52
$T_c^{**}(h)$	+4.16	+0.72	—0.62	—2.58	—1.68	—1.33

* Model A.
** Model B.

digitation. The set of phases obtained from strip models are (+, +, −, −, −, −), for the first six reflections, the origin is at the center between adjacent head groups. The Fourier series representation $t(x)$ [28] is defined as follows:

$$t(x) = (2/d) \sum_{h=1}^{h=h_{max}} \{\pm\} |T_{obs}(h)| \cos 2\pi hx/d$$

The Fourier synthesis for the sphingomyelin bilayers was computed using $h_{max} = 6$ and the above phases and is shown in Fig. 3. The Fourier synthesis has a resolution of about 6 Å. The electron density profile has a single peak in the polar regions and it has a relatively uniform density in the hydrocarbon chain region and a small dip in electron density at $d/2$.

(2) Direct analysis using deconvolution. The Patterson function [28] is defined as follows:

$$P(x) = (2/d) \sum_{h=1}^{h=h_{max}} |T_{obs}(h)|^2 \cos 2\pi hx/d \, .$$

The Patterson function of sphingomyelin bilayers was computed using first six lamellar reflections, $h_{max} = 6$. The Patterson function was normalized so that $P(0) = 1$, and is shown in Fig. 4. At this resolution the Patterson function of sphingomyelin shows only one peak at about $x = 14$ Å.

During the course of this work it was realized that the interpretation of the

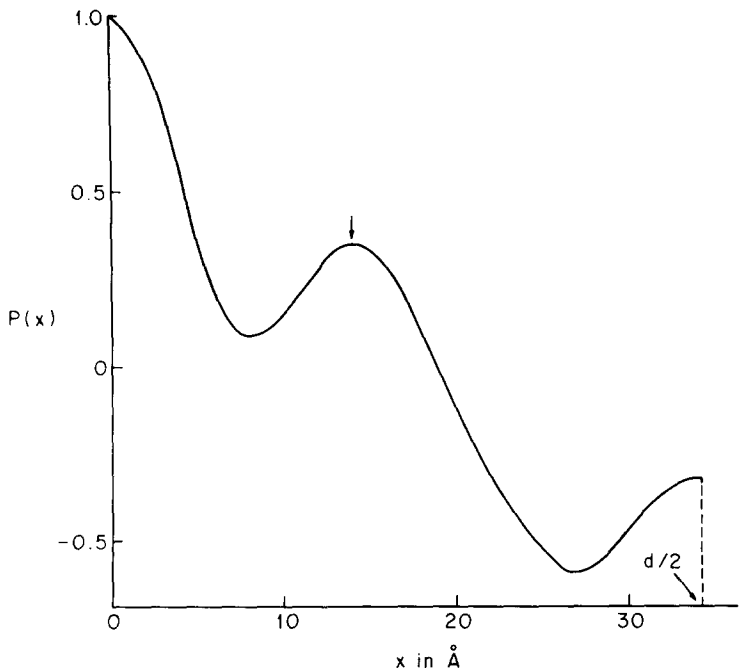

Fig. 4. Patterson function of sphingomyelin bilayers computed using the first six orders of diffraction. The arrow indicates a single peak in $P(x)$ at $x = 14$ Å.

Patterson function can be generalized in the sense that the phases can be obtained directly by deconvolution of the autocorrelation function [30] by assuming that the hydrocarbon region in the lipid bilayers has uniform electron density [31]. The diffraction theory of deconvolution of the autocorrelation function has been presented [30,32]. The theory of this deconvolution as applied to oriented lipid bilayers has been described [31,33] and only a short account is given here.

The autocorrelation function $A(x)$ and the Patterson function are related by

$$A(x) = K[P(x) - P(v)]$$

where K is the normalization constant and v is the width of the polar region. The autocorrelation function $A(x)$ can be computed from the Patterson function $P(x)$ by using the above relation, provided a correct choice of v can be made. The correctness of the choice of v can be examined by computing the Fourier transform of $A(x)$, which is $J_c(X)$, the continuous intensity transform, and

$$J_c(X) = 2 \int_0^v A(x) \cos 2\pi Xx \, dx$$

The intensity transform $J_c(X)$ for a particular value of v was computed from the above relation and then $J_c(h)$ and $J_{obs}(h)$ values were compared using an agreement index AI, where

$$AI = \frac{\sum_{h=1}^{h=h_{max}} |J_c(h) - J_{obs}(h)|}{\sum_{h=1}^{h=h_{max}} J_{obs}(h)}$$

The AI values were obtained for a range of v values in order to determine an initial estimate of parameter v. The AI values for v = 19, 21, 22, 23, and 25 Å are listed in Table II. The choice of v = 23 Å had the lowest AI value of 17%.

The deconvolution of $A(x)$ was carried out using the recursion method [30,32] to yield $s(x)$, the electron density distribution in the polar region of the bilayer. A Fourier transformation of $s(x)$ leads to a first estimate of the phases of the lower order reflections. This direct analysis gave the same set of phases for the first six reflections as was obtained using the electron strip models. The R values for the five solutions $s(x)$ obtained using the five choices of v are listed in Table II. The choice of v = 22 Å had the lowest R value of 24%.

TABLE II

AI AND *R* VALUES FOR FIVE CHOICES OF v

v (Å)	19	21	22	23	25
AI (%)	55.8	41.6	28.6	17.0	17.5
R (%)	32.5	24.6	23.9	25.0	30.4

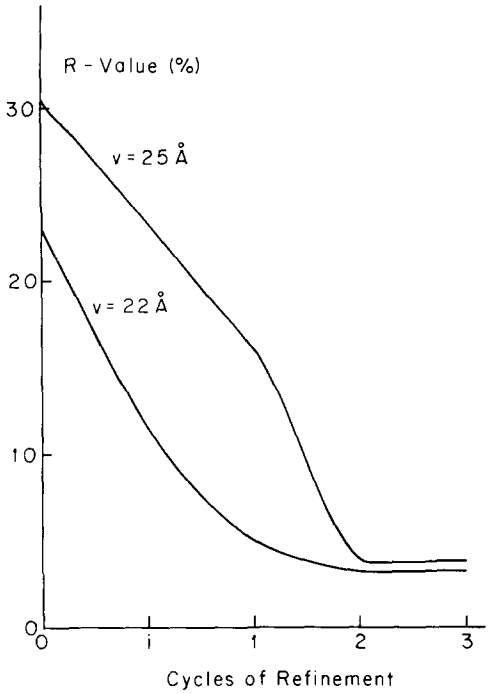

Fig. 5. The variation of the R value (%) for three cycles of refinement. The zero cycle refers to the initial deconvolution, i refers to the improved model and 1, 2 and 3 are cycles of refinement.

The direct analysis used so far assumes that the electron density in the hydrocarbon region is fairly uniform and the width of the polar region $v < d/2$. The assumption of constant electron density in the hydrocarbon region is an approximation to the true structure since Fourier profiles for lipid bilayers show a dip in electron density centered in the hydrocarbon region. Therefore, a refinement of the deconvolution method which allows for this dip in the hydrocarbon region was adopted [33]. An improved model was derived from a comparison of $s(x)$ and the Fourier profile computed by using the first estimate of phases and observed amplitudes, and including a dip in electron density of overall width w and depth g relative to the peak height of the polar region density and centered at $x = \pm d/2$. This model was used to obtain a new auto-correlation function and a cyclic refinement of the bilayer model was carried out [33].

Two cycles of refinement of the improved model gave the same set of phases as obtained by electron density strip model analysis. Variation of R values with cycles of refinement, starting with two choices of v, $v = 22$ Å and $v = 25$ Å, is shown in Fig. 5. The R values dropped from about 30% to about 5% and in both cases a final value of $v = 22$ Å was obtained using parameters $g = 0.32$ and $w = 11$ Å.

(B) High resolution analysis

(1) Patterson function. The Patterson function of sphingomyelin bilayers

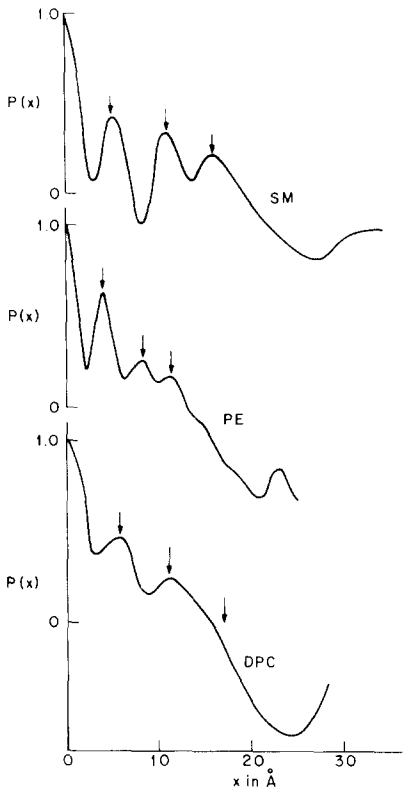

Fig. 6. Patterson functions of sphingomyelin (SM) bilayers phosphatidylethanolamine (PE) bilayers and phosphatidylcholine (DPC) bilayers. The Patterson functions were computed using the first 14 orders of diffraction for sphingomyelin, the X-ray data of Hitchcock et al. [19] was used for phosphatidylethanolamine and the X-ray data of Torbet and Wilkins [16] was used for phosphatidylcholine. The arrows indicate three peaks in $P(x)$ at x = 5, 11 Å and x = 16 Å for sphingomyelin. Similarly, arrows indicate three peaks at x = 4 Å, x = 7.2 Å and x = 11.2 Å for phosphatidylethanolamine while for phosphatidylcholine the three peaks are at x = 5.7 Å, x = 11 Å and at x = 17 Å (which is just discernible).

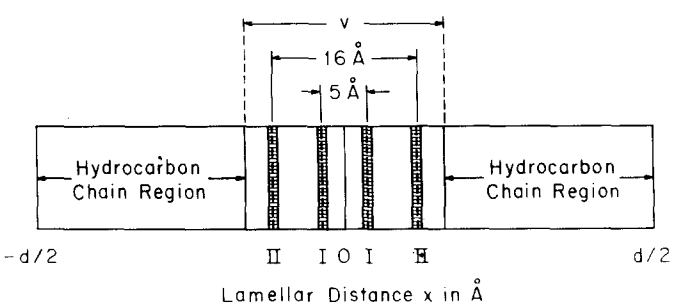

Fig. 7. A schematic drawing of the two high density centers, I and II, in the polar region of sphingomyelin bilayers: I is centered at x = ±2.5 Å and II at x = ±8 Å. The adjacent head groups have a width of v.

was computed using the first 14 lamellar reflections, $h_{max} = 14$, and is shown in Fig. 6. The Patterson function of sphingomyelin at this resolution has three well-resolved peaks at about 5, 11 and 16 Å and the minimum value of $P(x)$ is at about 27 Å. These three peaks in the Patterson function of sphingomyelin can be identified with two high electron density centers, denoted by I and II, in the polar region of the sphingomyelin bilayer as indicated in Fig. 7. We note that the I-I distance of 5 Å and the II-I distance of 5.5 Å accounts for the 5 Å peak, the (II-I) + (I-I) distance accounts for the 11 Å peak and the II-II distance accounts for the 16 Å peak.

It is instructive to examine the Patterson function of phosphatidylethanolamine as the structure of phosphatidylethanolamine is known [18,19]. The Patterson function of phosphatidylethanolamine was computed using the X-ray data [19] where $d = 49.5$ Å and $h_{max} = 15$. The Patterson function of phosphatidylethanolamine is shown in Fig. 6 and it has three well-resolved peaks at about 4, 7.2 and 11.2 Å. As in the case of sphingomyelin bilayers, these three peaks can be identified with two high electron density centers I and II, where I-I $\approx$ 4 Å and II-II $\approx$ 11.2 Å. It is known that the conformation of the polar group in phosphatidylethanolamine is in a compact form, bent normal to the plane of the bilayer [18], and the two high electron density centers in the Patterson function of phosphatidylethanolamine can, therefore, be attributed to the bent conformation of the polar head group in phosphatidylethanolamine bilayers. It suggests that the conformation of the polar group in sphingomyelin bilayer is also bent and is in the plane of the bilayer. The small differences in the position and amplitude of the peaks in the Patterson functions of sphingomyelin and phosphatidylethanolamine can be attributed to the difference in the size of the two polar groups: sphingomyelin having a $N^+(CH_3)_3$ group, phosphatidylethanolamine having a N^+H_3 group.

It is also instructive to examine the Patterson function of phosphatidylcholine as the structure of phosphatidylcholine at low humidity is known [14,16]. The Patterson function of phosphatidylcholine was computed using the X-ray data [16] where $d = 56.5$ Å and $h_{max} = 12$. The Patterson function of phosphatidylcholine is shown in Fig. 6 and it has two peaks at about $x = 5.7$ Å and $x = 11$ Å. There is a third peak at about $x = 17$ Å but this peak is poorly resolved and is only just descernible. Although the peaks in the Patterson function of phosphatidylcholine are not as well defined as in sphingomyelin and phosphatidylethanolamine, nevertheless, the similarity is apparent. The relative weaker peaks in phosphatidylcholine derive from the presence of a large dip in electron density at the center of the hydrocarbon chain. Thus, the peaks in the Patterson function of phosphatidylcholine are attributed to the bent conformation of the polar group in phosphatidylcholine bilayers and this conclusion is in agreement with the previous X-ray studies [16].

(2) Molecular model building. The determination of phases of the higher orders of diffraction from membranes is difficult even when accurate X-ray data has been obtained [34]. We have attempted to solve this problem by molecular model building. Our low resolution analysis suggested that the chains in sphingomyelin bilayers are straight and have very little interdigitation and the set of phases for the first six reflections is (+, +, —, —, —, —). Analysis of the Patterson function of sphingomyelin and a comparison with the Patterson

functions of phosphatidylethanolamine and phosphatidylcholine indicated a bent conformation for the polar head group in sphingomyelin bilayers. Based on this information, molecular models of sphingomyelin bilayers were built by computer simulation, using the published atomic coordinates for L-α-glycerophosphorylcholine [35], 1,2-dilauroyl-DL-phosphatidylethanolamine [18], triacetylsphingosine [36] and *N*-tetracosanoyl-phytosphingosine [37]. Atomic coordinates of sphingomyelin molecules were computed after the procedure of Thompson [38] by using the appropriate bond lengths, bond angles and dihedral angles obtained from the above-related compounds and by adjusting the dihedral angles so as to give a bilayer configuration for the two sphingomyelin molecules in the bilayer. The Fourier transform amplitude $T_c(h)$ of sphingomyelin molecules in the oriented bilayer was computed using the expression:

$$T_c(X) = \sum_{j=1}^{j=N} f_j(X) \cos 2\pi X x_j ,$$

where N is the number of atoms in the unit cell, $f_j(X)$ is the atomic scattering factor [39] for the j^{th} atom at a distance X in the reciprocal space and x_j is the distance of the j^{th} atom from the origin $x = 0$. Hydrogen atoms were not included in these computations. Fourier transform values for the lamellar reflections $T_c(h)$ were compared with the experimental values $T_{obs}(h)$ and the R values for the various molecular configurations were computed. Typical R values for a 2, 4 and 6 Å interdigitation of the hydrocarbon chains were 60, 72, and 71%, respectively. A minimum R value of 37% was obtained when there was no interdigitation of the hydrocarbon chains of the two sphingomyelin molecules in the bilayer. A schematic drawing of this model is shown in Fig. 8 where only the half unit cell is illustrated. The observed $T_{obs}(h)$ and calculated Fourier transform values $T_c(h)$ for this model are listed in Table III. Note that the third reflection is given as having a (±) phase as the molecular model gave a (+) phase for $h = 3$, but, it was decided to use a (—) phase because the low resolution analysis indicated that the $h = 3$ reflection had a (—) phase. This issue was not studied further primarily because the $h = 3$ reflection had only a weak intensity and also because the computing was time-consuming. The phases (+) for $h = 1$ and 2 and (—) for $h = 3$—14 were obtained from molecular model building. These same phases for sphinogmyelin bilayers were the same as given by the electron density strip model B in Fig. 2. We note that the phases derived here for sphingomyelin bilayers are the same as derived for phosphatidylethanolamine bilayers [19].

A Fourier synthesis for the sphingomyelin bilayers was computed using the first 14 reflections and the set of phases, (+) for $h = 1$ and 2 and (—) for $h = 3$—14, and this Fourier which had a resolution of about 2.5 Å is shown in Fig. 8. The high resolution electron density profile of sphingomyelin has two well-defined peaks in the polar region and an extended hydrocarbon region. The two peaks can be identified with the folded phosphorylcholine group and the amide and hydroxyl groups in the polar region of the sphingomyelin. The ripple contour in the hydrocarbon region is consistent with the Fourier profile having a resolution of 2.5 Å, and indicates that the hydrocarbon chain region

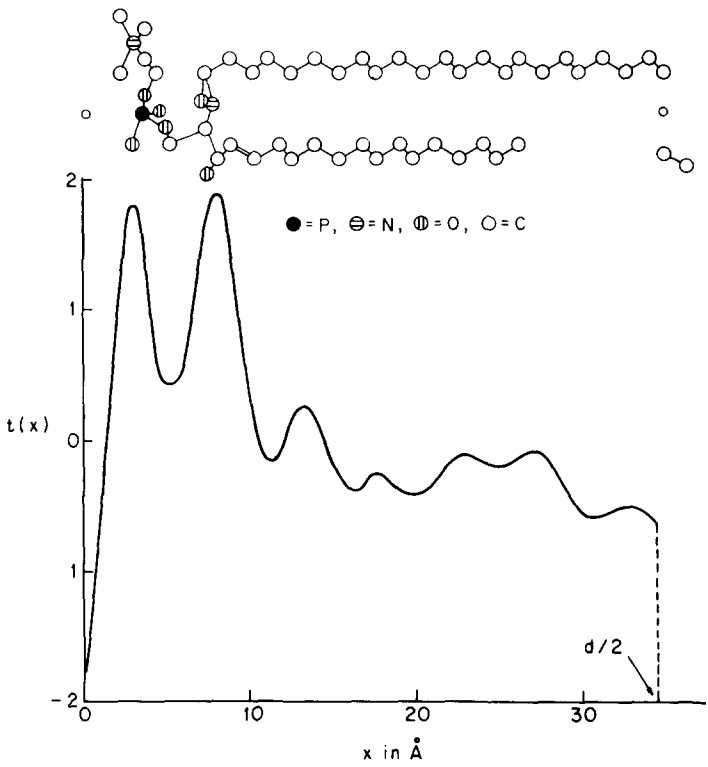

Fig. 8. The projection of a sphingomyelin molecule in the half unit cell with the molecular arrangement which gave the *R* value of 37% is shown at the top of the figure. In the lower half of the figure, the electron density profile of sphingomyelin bilayers computed using the first 14 orders of diffraction and (+) phases for $h = 1$ and 2 and (—) phases of $h = 3$—14 is shown. The Fourier synthesis is on a relative scale and has a resolution of about 2.5 Å. The molecular model for sphingomyelin at the top of the figure correlates with the Fourier profile.

TABLE III

THE OBSERVED AND CALCULATED FOURIER TRANSFORM VALUES FOR SPHINGOMYELIN BILAYERS

The calculated values were derived from the molecular model shown in Fig. 8.

h	$\lvert T_{obs}(h)\rvert$	$T_c(h)$
1	4.12	+5.02
2	0.74	+2.96
3	0.55	±0.63
4	2.74	—0.99
5	1.56	—1.51
6	1.36	—1.17
7	1.22	—0.58
8	0.44	—0.30
9	061	—1.51
10	0.78	—1.45
12	2.34	—1.67
13	2.64	—1.70
14	1.64	—1.60

has a relatively uniform density apart from the dip in electron density at the center of the hydrocarbon chain region. The relatively low electron density region of about 6 Å on either side of $d/2$ in the center of the bilayer can be attributed to the differences in the lengths of the amide fatty acid chain and the shorter sphinosine chain. It can be argued that, if the chains were fully extended, the low electron density region would be about 10 Å long. But a region of 6 Å was obtained and this could imply that the longer amide fatty acid chain was bent near the amide group. The relatively low electron density between the polar head groups of the two adjacent sphingomyelin molecules is in agreement with the bent conformation of the polar group, for extended and overlapping polar groups would have a much higher electron density. The electron density profile in Fig. 8 is consistent with the superimposed molecular model of sphingomyelin.

Discussion

The X-ray analysis of the lamellar diffraction from sphingomyelin bilayers has been carried out at low resolution (6 Å) and at high resolution (2.5 Å). The phases for the first six reflections (low resolution) have been established using electron density strip models and direct deconvolution analysis. The phases for the reflections $h = 7—14$ (high resolution) have been obtained using molecular model building calculations and electron density strip models. The phases for the higher orders of diffraction are not as firmly established as the phases for the first six reflections.

The electron density profile of sphingomyelin bilayers at 2.5 Å resolution (Fig. 8) shows two peaks at $x \approx 3$ Å and at $x \approx 8$ Å in the polar region of the sphingomyelin molecule and these two peaks are consistent with the peaks in the Patterson function (Fig. 6) at $x = 5$ Å, $x = 11$ Å, $x = 16$ Å. The polar region in Fig. 8 extends to $x \approx 11$ Å in agreement with the value of $v = 22$ Å which was obtained by deconvolution analysis. The molecular model for sphingomyelin (Fig. 8) has a bent polar head group which lies in the plane of the bilayer. The low density region at $x = 0$ between adjacent head groups is also consistent with the bent conformation of the head group for an extended conformation would have a much higher electron density between adjacent sphingomyelin molecules.

It is known from X-ray studies [16,18,19] that the polar head groups of phosphatidylethanolamine and phosphatidylcholine in oriented bilayers have a bent conformation and lie in the plane of the bilayer surfaces. The similarity between the Patterson functions of sphingomyelin, phosphatidylethanolamine and phosphatidylcholine is striking and is consistent with the bent conformation of the head group in three cases. The phases for sphingomyelin as derived here are the same as the phases given for phosphatidylethanolamine [19] and, although there are differences in repeat distances, lengths of hydrocarbon chains and in the head groups, spingomyelin and phosphatidylethanolamine have the same kind of molecular arrangement. On the other hand, although sphingomyelin and phosphatidylcholine have somewhat different head groups, nevertheless, they have the same phosphorylcholine polar group and, as the Patterson peaks for sphingomyelin and phosphatidylcholine occur at $x \approx 5$ Å,

$x \approx 11$ Å and $x \approx 17$ Å for both the conformation of the head groups of sphingomyelin and phosphatidylcholine are very similar. Note that the Patterson peaks for phosphatidylcholine are not as well-defined as in sphingomyelin due to the presence of a pronounced dip in electron density at the center of the hydrocarbon chain region.

The experimental result that sphingomyelin bilayers did not swell with increase in humidity is noted. This result was not anticipated for sphingomyelin has the same phosphorylcholine polar group as phosphatidylcholine and the repeat periods of phosphatidylcholine are know to increase as the humidity is raised [11—16]. But sphingomyelin like phosphatidylethanolamine [17] did not swell when exposed to high humidities.

The X-ray analysis of the lamellar diffraction from sphingomyelin bilayers indicates that the hydrocarbon chains have uniform electron density along their length. The electron density strip models (Fig. 2), the molecular model building (Fig. 8), the Fourier profile and the molecular model shown in Fig. 8 provide evidence that the hydrocarbon chains are straight and parallel to each other. The 4.2 Å reflection which is characteristic of hydrocarbon chain packing in crystalline paraffins is arced on the equator and, hence, it can be argued tha the hydrocarbon chains are at right angles to the bilayer surface although there is some disorder.

The electron density dip at the center of the hydrocarbon chain region, $x = \pm d/2$, in sphingomyelin is similar to phosphatidylethanolamine but quite different from phosphatidylcholine. Phosphatidylcholine has two lipid chains of equal length and has a comparatively large dip in electron density attributed to the localization of the methyl groups [12]. The dip in electron density at $x = \pm d/2$ in sphingomyelin, phosphatidylethanolamine and natural membranes [34] is much smaller than in phosphatidylcholine for the reason that the lipid chains have unequal lengths.

The differences in the lengths of the two lipid chains of sphingomyelin suggests the possibility that the hydrocarbon chains of sphingomyelin are interdigitated in the bilayer. But, any interdigitation has to be small because of the large repeat distance of 68.5 Å. The X-ray analysis described here confirms that the hydrocarbon chains in sphingomyelin bilayers have very little, if any, interdigitation. This observation is in agreement with previous X-ray studies on phosphatidylethanolamine [19]

In summary, low angle X-ray diffraction patterns have been recorded from oriented sphingomyelin bilayers *. The phases of X-ray reflections have been determined using three different methods: strip models, molecular model building and by deconvolution. An electron density profile for sphingomyelin bilayers at about 2.5 Å resolution has been described. As a result of this X-ray analysis we find that the phosphatidylcholine head group of sphingomyelin is in the plane of the bilayer surface and at right angles to the hydrocarbon chains, the hydrocarbon chains in sphingomyelin bilayers are nearly stringht

* Since submitting this manuscript we have learned from Dr. J. Torbet that he has carried out an X-ray diffraction analysis on the structure of oriented bilayers of sphingomyelin [40]. Similar diffraction patterns were obtained although there were differences in experimental method. Torbet [40] describes possible model structures for sphingomyelin which are quite similar to the molecular model in Fig. 8. Thus, the two X-ray studies are confirmatory to each other.

and parallel to each other and there is very little interdigitation of the hydrocarbon chains of the sphingomyelin molecules in the bilayer.

Acknowledgements

This work was supported by a grant from the U.S. Public Health Service. Silane coupling agent was a gift from Dr. E. Plueddemann of Dow Corning Corp.

References

1 Strickland, K.P. (1973) in Form and Function of Phospholipids (Ansell, G.B., Hawthorne, J.N. and Dawson, R.M.C., eds.), pp. 9–41, Elsevier, Amsterdam
2 Burton, R.M. (1967) in Lipids and Lipodoses (Schettler, G., ed.), pp. 122–167, Springer-Verlag, New York
3 van Deenen, L.L.M. (1965) Prog. Chem. Fat Other Lipids 8, 1–127
4 Shah, D.O. and Schulman, J.H. (1967) Biochim. Biophys. Acta 135, 184–187
5 Sundaraligam, M. (1972) Ann. N.Y. Acad. Sci. 195, 324–355
6 Shipley, G.G., Avecilla, L.S. and Small, D.M. (1974) J. Lipid Res. 15, 124–131
7 Barenholz, Y., Suurkuus, J., Mountcastle, D., Thompson, T.E. and Biltonen, R.L. (1976) Biochemistry 15, 2441–2447
8 Wong, W.M. and Geil, P.H. (1976) Mol. Cryst. Liq. Cryst. 37, 281–301
9 Luzzati, V. and Tardieu, A. (1974) Ann. Rev. Phys. Chem. 25, 79–94
10 Khare, R.S. and Worthington, C.R. (1977) Mol. Cryst. Liq. Cryst. 38, 195–206
11 Levine, Y.K., Bailey, A.I. and Wilkins, M.H.F. (1968) Nature 220, 577–578
12 Levine, Y.K. and Wilkins, M.H.F. (1971) Nat. New Biol. 230, 69–72
13 SAkurai, I., Iwayanagi, S., Sakuri, T. and Seto, T. (1977) J. Mol. Biol. 117, 285–291
14 Lesslauer, W., Cain, J.E. and Blasie, J.K. (1972) Proc. Natl. Acad. Sci. U.S. 69, 1499–1503
15 Powers, L. and Clark, N.A. (1975) Proc. Natl. Acad. Sci. U.S. 72, 840–843
16 Torbet, J. and Wilkins, M.H.F. (1976) J. Theor. Biol. 62, 447–458
17 Green, J.P., Phillips, M.C. and Shipley, G.G. (1973) Biochim. Biophys. Acta 330, 243–253
18 Hitchcock, P.B., Mason, R., Thomas, K.M. and Shipley, G.G. (1975) Proc. Natl. Acad. Sci. U.S. 71, 3036–3040
19 Hitchcock, P.B., Mason, R. and Shipley, G.G. (1975) J. Mol. Biol. 94, 297–299
20 Bear, R.S., Palmer, K.J. and Schmitt, F.O. (1941) J. Cell Comp. Physiol. 17, 355–367
21 Finean, J.B. (1953) Biochim. Biophys. Acta 10, 371–384
22 Reiss-Husson, F. (1967) J. Mol. Biol. 25, 363–382
23 Khare, R.S., Mishra, R.K., Falor, W.H. and Geil, P.H. (1974) Indian J. Biochem. Biophys. 11, 327–330
24 Khare, R.S. and Worthington, C.R. (1976) Biophys. J. 16, 137a
25 Elliott, G.F. and Worthington, C.R. (1963) J. Ultrastruct. Res. 9, 166–170
26 Blaurock, A.E. and Worthington, C.R. (1966) Biophys. J. 9, 305–312
27 O'Brien, J.S. and Rouser, G. (1964) J. Lipid Res. 5, 339–342
28 Worthington, C.R. (1969) Biophys. J. 9, 222–234
29 Worthington, C.R. (1972) Ann. N.Y. Acad. Sci. 195, 293–307
30 Worthington, C.R., King, G.I. and McIntosh, T.J. (1973) Biophys. J. 13, 480–494
31 Khare, R.S. and Worthington, C.R. (1977) Biophys. J. 17, 50a
32 Hosemann, R. and Bagchi, S.N. (1962) in Direct Analysis of Diffraction by Matter, North-Holland Publishing Co., Amsterdam
33 Worthington, C.R. and Khare, R.S. (1978) Biophys. J. 23, 407–425
34 Worthington, C.R. (1973) Curr. Top. Bioenerg. 5, 1–39
35 Abrahamson, S. and Pascher, I. (1966) Acta Cryst. 21, 79–87
36 O'Connell, A.M. and Pascher, I. (1969) Acta Cryst. B25, 2553–2561
37 Dahlen, B. and Pascher, I. (1972) Acta Cryst. B28, 2396–2404
38 Thompson, H.B. (1967) J. Chem. Phys. 47, 3407–3440
39 Hubbell, J.H., Veigle, W.J., Briggs, E.A., Brown, R.T., Cromer, D.T. and Howerton, R.J. (1975) J. Phys. Chem. Ref. Data 4, 471–538
40 Torbet, J. (1973) Ph.D. Thesis, London University, London, England